

Effects of Quark–Pomeron Coupling Structure in Diffractive Deep Inelastic Scattering

S.V.Goloskokov,¹

Bogoliubov Laboratory of Theoretical Physics,
Joint Institute for Nuclear Research,
Dubna 141980, Moscow region, Russia

Abstract

We study the contribution of diffractive $Q\bar{Q}$ production to the F_2^D proton structure function and the longitudinal double-spin asymmetry in polarized deep-inelastic lp scattering. We show the strong dependence of the F_2^D structure function and the A_{ll} asymmetry on the quark–pomeron coupling structure.

¹Email: goloskkv@thsun1.jinr.dubna.su

1 Introduction

The diffractive events with a large rapidity gap between the final proton p' and the produced hadron system X in deep inelastic lepton–proton scattering

$$e + p \rightarrow e' + p' + X \quad (1)$$

have recently been studied in several experiments [1, 2]. The natural explanation of these events can be based on the hard photon–pomeron interaction. They can be interpreted as observation of the partonic structure of the pomeron [3]. Besides this effect, the contribution where all the energy of the pomeron goes into the $Q\bar{Q}$ production [4, 5] may be very important at small x_p (x_p is part of the momentum p carried off by the pomeron). This region is under investigation in the HERA energy domain.

The reaction (1) can be described in terms of the kinematic variables which are defined as follows:

$$Q^2 = -q^2, \quad t = (p - p')^2, \\ y = \frac{pq}{p_l p}, \quad x = \frac{Q^2}{2pq}, \quad x_p = \frac{q(p - p')}{qp}, \quad \beta = \frac{x}{x_p}, \quad (2)$$

where p_l, p'_l and p, p' are the initial and final lepton and proton momenta, respectively, $q = p_l - p'_l$.

The diffractive structure function $F_2^{D(4)}$ is related to the spin–average cross section of reaction (1)

$$\frac{d^4\sigma}{dx dQ^2 dx_p dt} = \frac{4\pi\alpha^2}{xQ^4} [1 - y + \frac{y^2}{2}] F_2^{D(4)}(x, Q^2, x_p, t). \quad (3)$$

Different models have been proposed to study the diffractive structure function F_2^D [6, 7]. As a rule, they are based on the assumption about the factorization at small x_p of F_2^D into the pomeron flux factor $f(x_p, t)$ and the pomeron structure function $F_2^P(\beta, Q^2, t)$

$$F_2^{D(4)}(x, Q^2, x_p, t) = f(x_p, t) F_2^P(\beta, Q^2, t). \quad (4)$$

The partonic interpretation is usually used for the pomeron structure function $F_2^P(\beta, Q^2, t)$ [8].

The function $f(x_p, t)$ at small x_p behave as [6]

$$f(x_p, t) \propto \frac{1}{x_p^{2\alpha_P(t)-1}}, \quad (5)$$

where $\alpha_P(t)$ is the pomeron trajectory

$$\alpha_P(t) = \alpha_P(0) + \alpha' t, \quad \alpha' = 0.25(GeV)^{-2}. \quad (6)$$

The data on F_2^D [1, 2] can be fitted by the single exponent x_p^{-N} where

$$N \simeq \begin{array}{ll} 1.2 \pm 0.1 & \text{for H1} \\ 1.3 \pm 0.1 & \text{for ZEUS} \end{array} \quad (7)$$

are independent of β and Q^2 . This behaviour is consistent with the "soft" pomeron [6, 9] with $\alpha_P(0) = 1.1 - 1.15$. The hard perturbative pomeron [10] leads to $N \simeq 2$ that is in contradiction with HERA diffractive experiments.

Pomeron is a colour singlet state which is associated in QCD with the two-gluon exchange [11]. Gluons from the pomeron can interact with a single quark in the loop, which leads to planar contributions. There are nonplanar graphs in which gluons from the pomeron interact with different quarks in the loop. Such effects, as a rule, do not exceed 10 per cent as compared to the planar-diagram contributions (see e.g. [12]). Moreover, it can be shown [13] that the nonplanar effects should be important at large momentum $k_\perp^2 \sim Q^2/\beta$. The contribution of this region to the cross-section is rather small. As a result, the pomeron should prefer to interact with a single quark in the loop. Thus, we can use the effective quark-pomeron vertex in our calculations.

The diffractive scattering of polarized particles is proposed to be studied at HERA and RHIC [14]. Then, the question of how large the spin-flip component of the pomeron should be very important. In the nonperturbative two-gluon exchange model [15] and the BFKL model [10] the pomeron couplings have a simple matrix structure (the standard coupling in what follows):

$$V_{hhP}^\mu = \beta_{hhP} \gamma^\mu. \quad (8)$$

In this case, the spin-flip effects are suppressed as a power of s .

The situation does change drastically when the large-distance loop contributions are considered, which complicates the spin structure of the pomeron coupling. These effects can be determined by the hadron wave function for the pomeron-hadron couplings. The spin-flip effects that do not vanish as $s \rightarrow \infty$ have been found in some models of high-energy hadron scattering [16, 17]. In the model [17] the pomeron-proton vertex has the form

$$V_{ppP}^\mu(p, r) = mp^\mu A(r) + \gamma^\mu B(r), \quad (9)$$

where m is the proton mass. The coupling (9) leads to the spin-flip in the pomeron exchange.

The spin structure of quark-pomeron coupling may not be so simple too. It has been shown that the perturbative gluon loop corrections modify the form of the quark-pomeron coupling which looks like

$$V_{qqP}^\mu(k, r) = \beta_{qqP} [\gamma^\mu + 2M_Q k^\mu u_1 + 2k^\mu \not{k} u_2 + iu_3 \epsilon^{\mu\alpha\beta\rho} k_\alpha r_\beta \gamma_\rho \gamma_5 + iM_Q u_4 \sigma^{\mu\alpha} r_\alpha], \quad (10)$$

where k is the quark momentum, r is the momentum transfer and M_Q is the quark mass. So, in addition to the γ_μ term, the new structures appear from the loop diagrams. The functions $u_1(r) - u_4(r)$ are proportional to α_s . It has been shown [18] that these functions can reach 20 – 30% of the standard pomeron term $\sim \gamma_\mu$ for $|r^2| \simeq \text{few } \text{GeV}^2$. Note that the modified quark-pomeron coupling (10) is drastically different from the standard one (8). Really, the terms $u_1(r) - u_4(r)$ lead to the spin-flip at the quark-pomeron vertex in contrast with the term γ_μ . We shall call the form (10) the spin-dependent pomeron coupling. The phenomenological vertex V_{qqP}^μ with the γ_μ and u_1 terms was proposed in [19]. The modification of the standard pomeron vertex (8) might be obtained from the instanton contribution [20].

Thus, the pomeron couplings may have a complicated spin structure. As a result, the spin asymmetries appear which have weak energy dependences as $s \rightarrow \infty$.

In this paper, we study the effects of the spin-dependent quark-pomeron coupling in diffractive deep inelastic scattering. We perform the perturbative calculation of the diffractive $Q\bar{Q}$ production to the process (1) determined by Fig.1. We investigate unpolarized and polarized lepton-proton deep inelastic scattering that can be analyzed in future polarized experiments at HERA.

In the second part of the paper, we study the diffractive contribution to the F_2 structure function. In the third part, we calculate the distribution of spin-dependent cross sections and double-spin longitudinal asymmetry over the transverse momentum of a produced jet. It is shown that all these effects are sensitive to the quark-pomeron coupling structure.

2 $F_2^{D(3)}$ diffractive structure function

Let us study the diffractive jet production using expression (10) as the effective quark-pomeron coupling. The term $\gamma^\mu B(r)$ in the proton-pomeron coupling (9) gives the predominated contribution to the cross sections for the spin-average and longitudinal polarization of the proton. Thus, in what follows we shall use the standard form of the pomeron-proton coupling (8). The spin-average cross section of the reaction (1) can be written in the form (3) where the diffractive structure function looks like

$$F_2^{D(4)}(x, Q^2, x_p, t) = \beta \frac{3\beta_0^4 F(t)^2 [9 \sum_i e_i^2]}{1024\pi^4 x_p} I(\beta, Q^2, x_p, t), \quad (11)$$

$$I(\beta, Q^2, x_p, t) = \int_{k_0^2}^{Q^2/4\beta} \frac{dk_\perp^2 N(\beta, k_\perp^2, x_p, t)}{\sqrt{1 - 4k_\perp^2 \beta / Q^2 (k_\perp^2 + M_Q^2)}}. \quad (12)$$

Here M_Q is the quark mass, β_0 is the quark-pomeron coupling, $F(t)$ is the pomeron-proton form factor, e_i are the quark charges. The integral $I(\beta, Q^2, x_p, t)$ represents the contribu-

tions of the box diagram of Fig.1 and the corresponding crossed graph. The function N is determined by the trace over the quark loop. It can be written for $x_p = 0$ in the form

$$N(\beta, k_\perp^2, t) = N^s(\beta, k_\perp^2, t) + \delta N(\beta, k_\perp^2, t). \quad (13)$$

Here N^s is the contribution of the standard pomeron vertex (8) and δN contains the contribution of the $u_1(r) - u_4(r)$ terms from (10). The traces have been calculated by using the programme REDUCE. For the term N^s in the case of light quarks in the loop we find

$$N^s(\beta, k_\perp^2, t) = 32[2(1 - \beta)k_\perp^2 - \beta|t|]|t|. \quad (14)$$

The calculation of the δN term is difficult. We have found it in the $\beta \rightarrow 0$ limit. For the massless quarks only the u_3 terms contribute to δN :

$$\delta N(k_\perp^2, t) = 32k_\perp^2|t|[(k_\perp^4 + 4k_\perp^2|t| + |t|^2)u_3 - 4k_\perp^2 - 2|t|]u_3. \quad (15)$$

Note that δN is positive because $u_3 \leq 0$. Higher twist terms of an order of M_Q^2/Q^2 and $|t|/Q^2$ have been dropped in (14,15).

The k_\perp^2 dependence of the u_i functions, which is important in the calculation, has been studied. It was found that all functions decreased with growing k_\perp^2 . A good approximation of this behaviour is

$$u_i(k_\perp, r) = \frac{|t| + \mu_0}{k_\perp^2 + |t| + \mu_0} u_i(0, r), \quad r^2 = |t|, \quad \mu_0 \sim 1(\text{GeV})^2. \quad (16)$$

This improves the convergence of the integral over d^2k_\perp . The functions $u_i(0, r)$ in (16) are the corresponding form factors for the on-mass-shell quarks which have been calculated perturbatively [18]. The result of integration over d^2k_\perp in (12) is complicated in form and we do not show it here.

Expression (11) has been obtained for the pomeron with $\alpha_P(t) = 1$. For the supercritical pomeron with $\alpha_P(0) \geq 1$ we must replace the simple power x_p by the power $x_p^{2\alpha_P(t)-1}$. This behaviour of the diffractive cross section is connected with the pomeron flux factor (5).

Note that the momentum transfer t was not fixed in diffractive experiments [1, 2]. The integrated cross sections and diffractive structure function

$$F_2^{D(3)}(x, Q^2, x_p) = \int_{t_m}^0 dt F_2^{D(4)}(x, Q^2, x_p, t), \quad |t_m| = 7(\text{GeV})^2 \quad (17)$$

are used.

Let us determine the low- x_p behaviour of $F_2^{D(3)}$. We find from (11,13)

$$F_2^{D(4)}(x, Q^2, x_p, t) \sim \frac{te^{2bt}}{x_p^{2(\alpha_P(0)+\alpha'_P t)-1}} = \frac{te^{2t(b+\alpha'_P \ln 1/x_p)}}{x_p^{2\alpha_P(0)-1}}. \quad (18)$$

Here, the exponential form of the proton form factor $F(t) = e^{bt}$ with $b = 1.9(\text{GeV})^{-2}$ has been used. Integration over t in (17) gives us the following form of the $F_2^{D(3)}$ structure function at small x_p

$$F_2^{D(3)} \propto \frac{1}{x_p^{2\alpha_P(0)-1} (b + \alpha'_P \ln 1/x_p)^2}. \quad (19)$$

Using this equation we can evaluate the effective pomeron intercept from the fit (7)

$$\alpha_P(0) = \frac{N+1}{2} + \frac{\alpha'_P}{b + \alpha'_P \ln 1/x_p}. \quad (20)$$

We find for $x_p = 10^{-4} - 10^{-2}$

$$\alpha_P(0) \sim 1.15 - 1.2. \quad (21)$$

This value is a little larger than the standard pomeron intercept obtained from the elastic reactions [9] which is equal to $\alpha_P(0) = 1.08$. We think that this may be connected with the manifestation of the same pomeron in different regions of momentum transfer. In hard scattering processes, the interaction time is small and the single pomeron exchange with $\alpha_P(0) \sim 1.2$ contributes. In soft diffractive hadron reactions, the interaction time is large and the pomeron rescattering effects must be important. These contributions decrease the pomeron intercept to the standard value $\alpha_P(0) \sim 1.08$ [21]. The same point of view was expressed in [22].

In calculations, the perturbative results for the quark–pomeron vertex have been used. Note that in the integral (17) the integration region over t includes the range of small momentum transfer $|t| \leq 1(\text{GeV})^2$ where the nonperturbative effects should be important. However, the contribution of this range to the structure function is rather small because the function N in (13) is proportional to $|t|$. The results of calculations for the $F_2^{D(3)}$ structure function are shown in Fig.2 for $\alpha_P(0) = 1.1$. It can be seen from this figure that the diffractive contribution for the standard pomeron vertex is about 15 – 20% of the experimental results for $F_2^{D(3)}$, which coincides with the conclusion from [4, 6]. The contribution of the spin–dependent pomeron vertex increases the diffractive structure function by a factor of about two. As we have expected from (21), the experimental data have a much steeper x_p dependence for this $\alpha_P(0)$.

In Fig. 3, the results of calculations for $\alpha_P(0) = 1.15$ are shown. The shape of the obtained curves coincides with the x_p –dependence of experimental data. We find that the results of theoretical calculations for the spin–dependent pomeron vertex practically coincide in this case with experimental results. As previously, the predictions for the standard pomeron vertex lies lower than the curve for the spin–dependent pomeron vertex. Note that at small β the invariant mass of the produced system is large, and in addition to the effects of Fig.1 the triple pomeron contributions exist which should raise the diffractive $Q\bar{Q}$ production effects studied here up to experimental data (see e.g. [8]).

3 Spin-dependent Diffractive Deep Inelastic Scattering

Let us study now the spin-dependent cross sections and the longitudinal double spin A_{ll} asymmetry which is determined by the relation

$$A_{ll} = \frac{\Delta\sigma}{\sigma} = \frac{\sigma(\overset{\rightarrow}{\leftarrow}) - \sigma(\overset{\leftarrow}{\rightarrow})}{\sigma(\overset{\rightarrow}{\rightarrow}) + \sigma(\overset{\leftarrow}{\leftarrow})}, \quad (22)$$

where $\sigma(\overset{\rightarrow}{\rightarrow})$ and $\sigma(\overset{\rightarrow}{\leftarrow})$ are the cross sections with parallel and antiparallel longitudinal polarization of lepton and proton.

The A_{ll} asymmetry for the integrated cross sections over the transverse momentum of the produced jet have been calculated in [23]. It was found that the asymmetry was dependent on the quark-pomeron coupling structure and could reach 10 – 20%.

Here, we shall calculate perturbatively the distribution of the diffractive deep inelastic cross section over the transverse momentum of the produced jet k_{\perp}^2 . The difference of the cross section for the supercritical pomeron can be written in the form

$$\Delta\sigma(t) = \frac{d^5\sigma(\overset{\rightarrow}{\leftarrow})}{dx dy dx_p dt dk_{\perp}^2} - \frac{d^5\sigma(\overset{\leftarrow}{\rightarrow})}{dx dy dx_p dt dk_{\perp}^2} = \frac{3(2-y)\beta_0^4 F(t)^2 [9 \sum_i e_i^2] \alpha^2}{128 x_p^{2\alpha_P(t)-1} Q^2 \pi^3} \frac{A(\beta, k_{\perp}^2, x_p, t)}{\sqrt{1 - 4k_{\perp}^2 \beta / Q^2 (k_{\perp}^2 + M_Q^2)^2}}. \quad (23)$$

The notation here is similar to that used in Eqs. (11,12).

The function A is connected with the trace over the quark loop. The leading x_p dependence is extracted in the coefficient of Eq. (23) which is determined by the pomeron flux factor. Thus, we can calculate the function A as $x_p \rightarrow 0$. It can be written as follows:

$$A(\beta, k_{\perp}^2, t) = A^s(\beta, k_{\perp}^2, t) + \delta A(\beta, k_{\perp}^2, t). \quad (24)$$

Here A^s is the contribution of the standard pomeron vertex (8) and δA is determined by the $u_1(r) - u_4(r)$ terms from (10).

The function A^s for the light quarks looks like

$$A^s(\beta, k_{\perp}^2, t) = 16(2(1-\beta)k_{\perp}^2 - |t|\beta)|t| \quad (25)$$

We have calculated δA in the $\beta \rightarrow 0$ limit. For the massless quarks we have

$$\delta A(\beta, k_{\perp}^2, t) = -16(3k_{\perp}^2 + 2|t|)k_{\perp}^2 |t| u_3. \quad (26)$$

The leading twist terms have been calculated here as in the previous section.

The spin-average cross section can be written in the form

$$\sigma(t) = \frac{d^5\sigma(\overset{\rightarrow}{\leftarrow})}{dx dy dx_p dt dk_{\perp}^2} + \frac{d^5\sigma(\overset{\leftarrow}{\rightarrow})}{dx dy dx_p dt dk_{\perp}^2} = \frac{3(1-y+y^2/2)\beta_0^4 F(t)^2 [9 \sum_i e_i^2] \alpha^2}{128 x_p^{2\alpha_P(t)} y Q^2 \pi^3} \frac{N(\beta, k_{\perp}^2, x_p, t)}{\sqrt{1 - 4k_{\perp}^2 \beta / Q^2 (k_{\perp}^2 + M_Q^2)^2}}, \quad (27)$$

where N is determined by Eg. (13).

It can be seen that σ has a more singular behaviour than $\delta\sigma$ as $x_p \rightarrow 0$. This is determined by the fact that the leading term in $\delta\sigma$ is proportional to $\epsilon^{\mu\nu\alpha\beta}r_{\beta}\dots \propto x_p p$. Similar is true for the lepton part of the diagram of Fig.1. As a result, the additional term yx_p appears in $\delta\sigma$.

As in the previous section, we shall calculate the cross section integrated over momentum transfer

$$\sigma[\Delta\sigma] = \int_{t_m}^0 dt \sigma(t)[\Delta\sigma(t)], \quad |t_m| = 7(GeV)^2. \quad (28)$$

The expressions for the standard pomeron coupling contributions to σ and $\Delta\sigma$ have been found for arbitrary β . However, the results for the spin-dependent part of the pomeron coupling have been obtained for $\beta = 0$. So, we shall calculate the cross sections and asymmetry for not very large $\beta = 0.175$. The results of calculation for the cross section of the light quark production in diffractive deep inelastic scattering for the pomeron with the usual intercept $\alpha_P(0) = 1.1$ and $y = 0.7$ are shown in Fig. 4 for the standard and spin-dependent pomeron couplings. The predicted cross sections are not small. The shape of both the curves is very similar and for the spin-dependent pomeron coupling the cross section is larger by a factor of about two, as previously.

The asymmetry in the diffractive $Q\bar{Q}$ production is shown in Fig. 5. It can be seen from the cross section (23,27) that the asymmetry for the standard quark-pomeron vertex is very simple in form

$$A_U = \frac{yx_p(2-y)}{2-2y+y^2}. \quad (29)$$

There is no any k_{\perp} and β dependence here. For the spin-dependent pomeron coupling the asymmetry is more complicated because of the different contributions in δA and δN proportional to k_{\perp}^2 . In this case the A_U asymmetry is smaller than for the standard pomeron vertex. Thus, one can use the A_U asymmetry to test the quark-pomeron coupling structure. Note that from $\Delta\sigma$ in (23) the diffractive contribution to the g_1 spin-dependent structure function can be determined [24]. The obtained low $-x$ behaviour of $g_1(x)$ has a singular form like $1/(x^{0.3} \ln^2(x))$ which is compatible with the SMC data for $g_1^p(x)$ [25].

4 Conclusion

Thus, we have found that the structure of the quark-pomeron coupling can affect spin average and spin-dependent cross section. From the analysis of the F_2^D structure function we have found that the slope of the HERA experimental data at small x_p leads to the pomeron intercept of about $\alpha_P(0) \sim 1.15$, which is a little larger than $\alpha_P(0) \sim 1.08$ for elastic reactions.

The spin-dependent form of V_{qqP} leads to increasing of the cross section by a factor of about two. However, the shape of the cross sections is very similar for the standard and spin-dependent pomeron vertices. As a result, it will be difficult to test the pomeron coupling structure from the analysis of the cross section. The A_{ll} asymmetry is more convenient for this purpose. The asymmetry is free from all normalization factors and sensitive to the dynamics of pomeron interaction. Moreover, we have a well-defined prediction for A_{ll} for the standard pomeron vertex. This conclusion is similar to the results of [13] where the single-spin asymmetry in the diffractive $Q\bar{Q}$ production has been studied.

It has been mentioned that at small β there is a contribution which is associated with the triple pomeron interaction. The relative role of the diffractive $Q\bar{Q}$ production and PPP contribution can be tested experimentally by the observation of two high- p_t jet events and events that have more than two jets.

So, in this paper the perturbative QCD analysis of the effects determined by the spin-dependent quark-pomeron coupling in the diffractive deep inelastic scattering has been done. The sensitivity of the spin dependent cross section to the quark-pomeron coupling structure has been found. The nonperturbative contribution might be important in these reactions too.

We can conclude that the investigation of the longitudinal double spin asymmetry and the cross section of the diffractive deep inelastic scattering can give important information about the complicated spin structure or the pomeron coupling. For testing the pomeron-proton vertex the transverse polarization of the proton target (beam) should be more relevant [13]. The HERA facilities to study properties of the pomeron can give a possibility to test the size of the spin-flip pomeron coupling.

The author expresses his deep gratitude to N.Akchurin, A.V.Efremov, G.Mallot, P.Kroll, W.-D.Nowak, A.Penzo, G.Ramsey, A.Schäfer, O.V.Teryaev for fruitful discussions.

References

- [1] ZEUS Collaboration, M.Derrick et al. Z.Phys. **C68** (1995) 569.
- [2] H1 Collaboration, T.Ahmed et al, Phys.Lett. **B348** (1995) 681.
- [3] G.Ingelman, P.E.Schlein, Phys.Lett. **B152** (1985) 256.
- [4] A.Donnachie, P.V.Landshoff, Phys.Lett. **B285** (1992) 172.
- [5] J.C.Collins, L.Frankfurt, M.Strikman, Phys.Lett. **B307** (1993) 161.
- [6] A.Donnachie, P.V.Landshoff, Nucl.Phys. **B303** (1988) 634.
- [7] M.G.Ryskin, S.Yu.Sivoklokov, A.Solano. In Proc. of Int. Conf. on Elastic and Diffractive Scattering, Ed. by H.M.Fried, K.Kang, C-I Tang, World Sci, 1993, p.181;
K.Goulianos, E-print hep-ph 9506360.
R.Fiore, L.L.Enkovszky, F.Paccanoni, E-print hep-ph 9602434;
- [8] W.Buchmüller, Phys.Lett. **B355** (1995) 573.
K.Golec-Biernat, J.Kwiecinski, **B355** (1995) 329.
- [9] A.Donnachie, P.V.Landshoff, Nucl.Phys. **B231** (1984) 189.
- [10] E.A.Kuraev, L.N.Lipatov, V.S.Fadin, Sov.Phys. JETP **44** (1976) 443;
Y.Y.Balitsky, L.N.Lipatov, Sov.J.Nucl.Phys. **28** (1978) 822.
- [11] F.E.Low, Phys.Rev. **D12** (1975) 163;
S.Nussinov, Phys.Rev.Lett. **34** (1975) 1286.
- [12] S.V.Goloskokov, J. Phys. **G19** (1993) 67.
- [13] S.V.Goloskokov, E-print hep-ph 9511382, to appear in Phys.Rev.
- [14] G.Bunce et al., Phys. World **3** (1992) 1.
W.-D.Nowak, in AIP conference proceedings 343 on High Energy Spin Physics, eds. K. J. Heller and S. L. Smith, Woodbury, NY (1995), p.412.
- [15] P.V.Landshoff, O. Nachtmann, Z.Phys. **C35** (1987) 405.
- [16] J.Pumplin, G.L.Kane, Phys.Rev. **D11** (1975) 1183;
C.Bourrely, J.Soffer, T.T.Wu, Phys.Rev. **D19** (1979) 3249;
B.Z.Kopeliovich, B.G.Zakharov, Phys.Lett. **B226** (1989) 156 .
- [17] S.V.Goloskokov, S.P.Kuleshov, O.V.Selyugin, Z.Phys. **C50** (1991) 455.

- [18] S.V.Goloskokov, O.V. Selyugin, Yad. Fiz. **57** (1994) 727.
- [19] J.Klenner, A.Schäfer, W.Greiner, E-print hep-ph 9409451.
- [20] A.E.Dorokhov, N.I.Kochelev, Yu.A.Zubov, Int.Journ.Mod.Phys. **A8** (1993) 603;
M.Anselmino, S.Forte, Phys.Rev.Lett. **71** (1993) 223.
- [21] S.V.Goloskokov, S.P.Kuleshov, O.V.Selyugin, Mod. Phys.Lett. **A10** (1995) 1959.
- [22] A.Donnachie, preprint M/C-TH 94/07, Manchester, 1994.
- [23] S.V.Goloskokov, E-prints: hep-ph 9506347; hep-ph 9509238.
- [24] S.V.Goloskokov, E-print: hep-ph 9604261.
- [25] SMC Collaboration, D.Adams et al., Phys. Lett. **B329** (1994) 339.

Figure captions

Fig.1 Diffractive $Q\bar{Q}$ production in deep inelastic scattering.

Fig.2 $Q\bar{Q}$ production contribution to the $F_2^{D(3)}$ diffractive structure function at small x_p . Theoretical curves are shown for $Q^2 = 25(GeV)^2$ and $\alpha_P(0) = 1.1$: solid line -for the standard quark-pomeron vertex; dot-dashed line -for the spin-dependent vertex. Data are from Ref. [2].

Fig.3 $Q\bar{Q}$ production contribution to the $F_2^{D(3)}$ diffractive structure function at small x_p . Theoretical curves are shown for $Q^2 = 25(GeV)^2$ and $\alpha_P(0) = 1.15$: solid line -for the standard quark-pomeron vertex; dot-dashed line -for the spin-dependent vertex. Data are from Ref. [2].

Fig.4 Distribution of σ over jets k_\perp^2 . Solid line -for the standard vertex; dot-dashed line -for the spin-dependent quark-pomeron vertex.

Fig.5 k_\perp^2 -dependence of A_{ll} asymmetry. Solid line -for the standard vertex; dot-dashed line -for the spin-dependent quark-pomeron vertex.

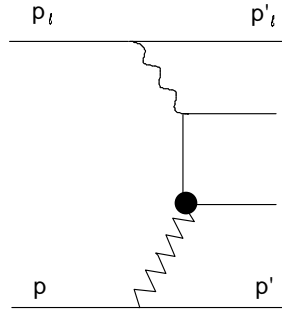


Fig.1

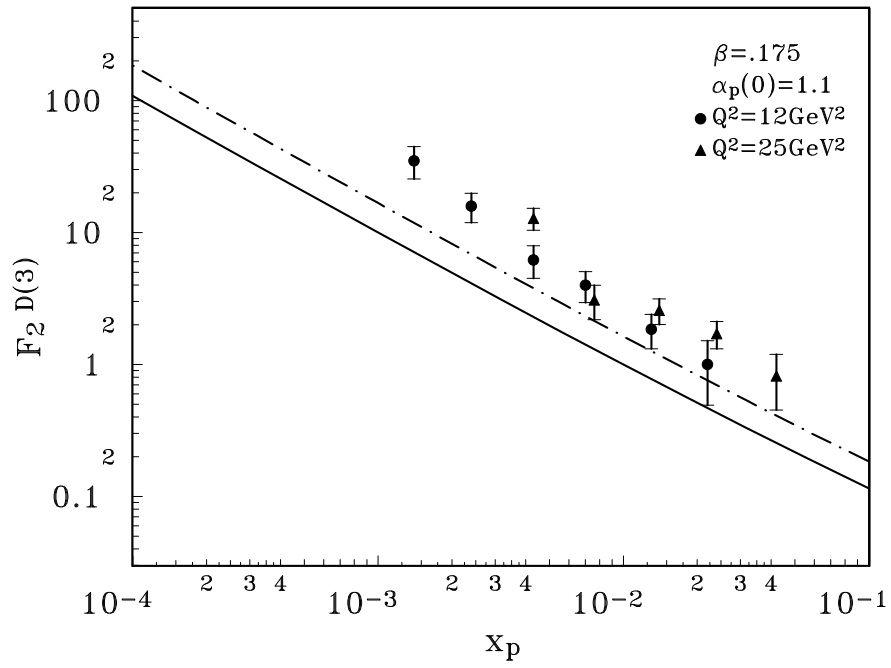


Fig.2

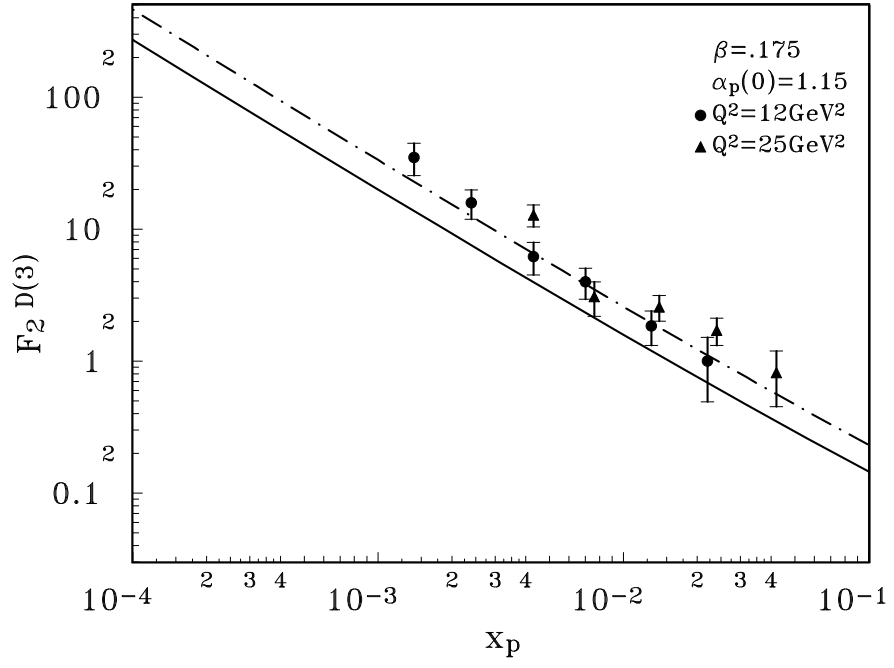


Fig.3

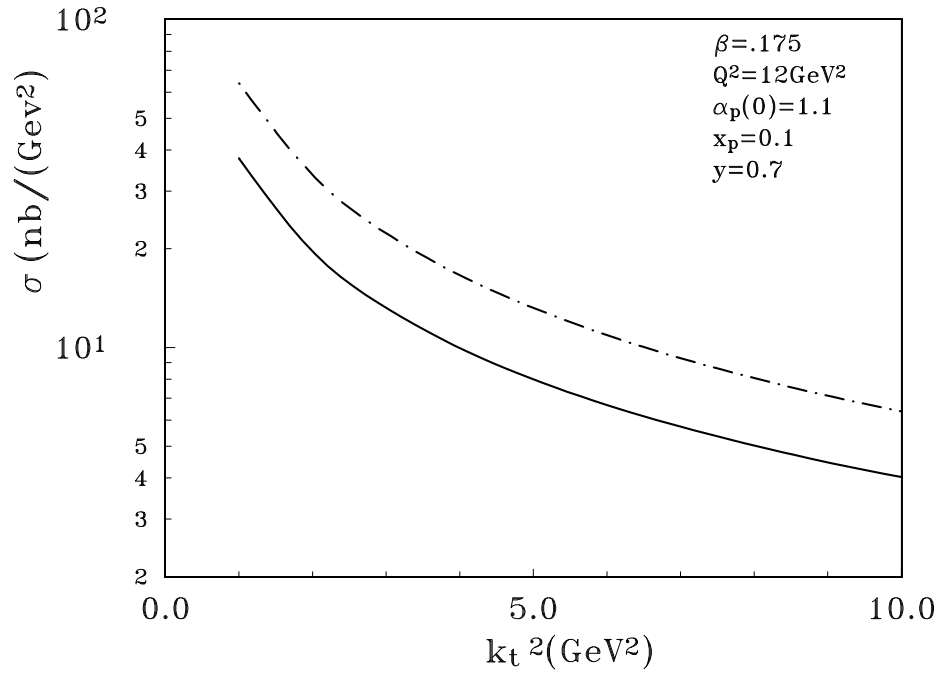


Fig.5

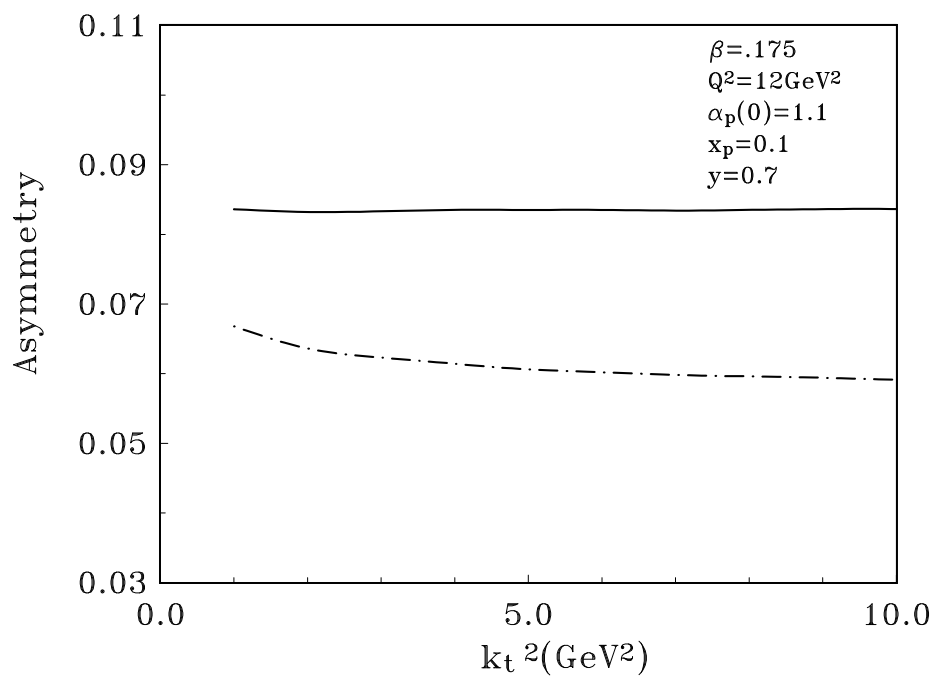


Fig.5